Parasitic Aware Routing Methodology based on Higher Order RLCK Moment Metrics

ABSTRACT

We propose a new routing methodology, which accounts for both inductive and capacitive coupling between neighboring wires. In the multi-GHz frequency domain, inductive parasitics of interconnects can cause significant signal deterioration and other effects like ringing that may lead to false switching and increased delay. Hence, routing techniques which rely on wire length reduction or coupling capacitance minimization are not sufficient to obtain the best routing solution. In this paper, the inductive and capacitive interactions of the wires are introduced through a 'moment' based cost function. This higher order RLCK moment metric guides the routing process thereby ensuring that the chosen solution has minimum ringing and delay under a monotone signal response. Another significant departure from existing routing methodologies is to account for the signal direction in the nets that may increase or decrease the effective inductive and capacitive parasitics. This routing methodology can be applied to MCM (multi-chip module) routing of long wires at high frequencies. Results show that the routing solutions obtained using our method achieves better signal quality and delay.

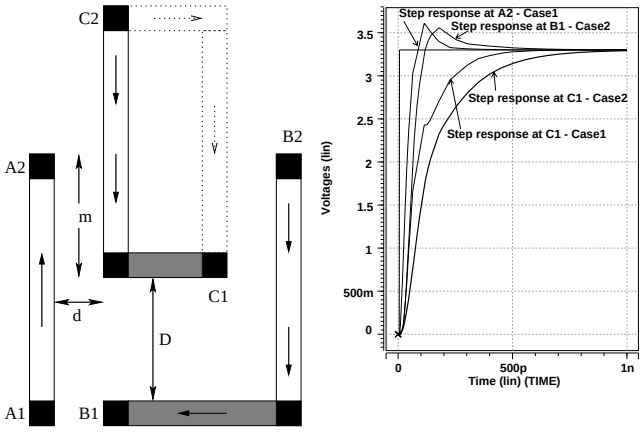

Figure 1: (A) Possible 1-bend routes (B) Signal Response at C1

1. INTRODUCTION AND MOTIVATION

In deep-submicron circuits, as the frequency of operation increases to the multi-GHz range, interconnect parasitics start playing a crucial role in circuit performance. Inductive and capacitive parasitics, both self and mutual, which were ignored in the realm of low-frequency designs, become important at high frequencies and are a dominant factor in determining interconnect delay and crosstalk of the circuit.

In traditional 'maze' routing it is difficult to introduce the effect of coupling parasitics. The maze router always finds the shortest path, which may lead to significant parallel runs between two neighboring wires giving rise to considerable amount of inductive and capacitive coupling. Recent crosstalk-aware routing methods [1] [2] have used coupling capacitance as a crosstalk measure. But, self and mutual inductive effects like ringing, can cause signal oscillations (overshoots and undershoots), leading to a greater settling time delay and distorted waveform response. We provide a motivating example in this regard.

In this simple example (Figure 1(A)), we consider only 1-bend routes ('L' shaped) for simplicity. We consider a situation when nets A1-A2 and B1-B2 have already been routed. We now try to determine the route for net C1-C2. There are two possible candidate routes for this net.

Case1: The lower-L route separated by distance 'd' that couples with A1-A2 for a length of 'm' and

Case2: The (dotted) upper-L route separated by distance 'd' that couples with B1-B2 for a length of 'm'.

(Note: the distance 'D' is greater than the threshold distance below which coupling is considered, hence the lower-L route does not couple with B1-B2).

As the coupling capacitance ($Cc \propto \frac{m}{d}$) is equal in both the cases, it becomes difficult to pick the best route from these two solutions. In our 'moment' driven routing cost function, we account for factors such as self and mutual inductance (L, K), direction of signal propagation, in addition to resistance (R) and self and coupling capacitance (C) between the neighboring wires. The 'RLCK' based moment metric then finds the best candidate route. In Figure 1(A) the current flows from A1 to A2, B2 to B1 and C2 to C1. In Case 1, we see that the current flows in opposite direction (odd-mode of propagation) and in Case2, the current flows in the same direction (even-mode of propagation). From the signal response at C1 in Figure 1(B), we observe that Case2 leads to a more overdamped response compared to Case1, leading to a greater net delay. Thus, Case1 (lower-L) is the better routing choice for net C1C2 as it's response is closer to the 'critically-damped' condition compared to Case2, leading to faster response. We also observe that the waveform response of A1-A2 is better than the response of B1-B2. In a contrasting situation when the current direction of net B1-B2 is reversed, an even-mode of current propagation occurs in both cases. Even in that situation, Case1 is chosen as the candidate route, since B1-B2 has a greater electrical length compared to A1-A2 that adversely affects the waveform response at C1.

In this paper, we propose a routing methodology driven by higher order 'moment-based' cost function. This cost function accounts for the R,L,C,K parasitics between neighboring wires and converges to a routing solution that minimizes the overall delay and results in a better waveform response for all the nets. The trade-off between delay and waveform response quality (amount of ringing) is well captured by means of a cumulative standard deviation of the second and third order moment metric of all the nets. A line-search

routing methodology has been used and customized to include our cost function. As our focus is to route wires connecting multi-chip modules (MCM) with long nets distributed over the entire silicon substrate, we do not use maze routing, due to its expensive memory requirements. We have considered 1-bend (L-shaped) and 2-bend (Z-shaped) routes for the nets in order to generate candidate routes and speed up the routing process [3].

2. RELATED WORK

There has been significant research in the field of area routing. The authors in [3] have used a simple congestion estimation technique in their global routing methodology. They have not allowed the number of route edges across a global bin edge exceed the edge capacity. Similar congestion estimation strategy have been used by the authors in [4], [5] with competing cost function formulation where the routing cost increased either linearly or abruptly with congestion. In [1] a routing technique has been proposed that is coupling aware only in terms of capacitance. Another work in the area of crosstalk reduction has been done in [2], [6] where the parasitic coupling capacitance occurs in the cost function formulation of the routing methodology and during layer track assignment respectively. The authors in [7], [8], [9] have developed various performance driven routing strategies using a simple Elmore (RC) delay model for the interconnects. Cong et al. [10], have used higher order RLC model in their MINOTAUR global router but they have not considered interwire inductive and capacitive coupling. Though all of the above routing methodologies have their own merits, none of them takes into consideration complete R,L,C,K parasitics during routing. We propose a routing methodology at multi-GHz frequency that will generate a solution considering the higher order R,L,C,K parasitics including inductive and capacitive coupling between neighboring wires. We also consider the relative signal direction between the aggressor and the victim nets to effectively capture the even and odd mode interwire interactions.

3. BACKGROUND INFORMATION

Our area routing methodology is governed by a cost function that is based on higher-order RLCK moment-metric. We will illustrate the key background concepts used to develop the route-cost.

***Ringing and Waveform Response*:** At high frequencies, the inductive effect of the interconnects gives rise to a transmission-line phenomenon called 'ringing' that adversely impacts the delay and signal quality by underdamping the waveform response. Ringing can inadvertently cause the circuit to transit to a wrong state and cause logic failure. This phenomenon is shown in Figure 2(C) and is well explained in [11]. Figure 2(C) shows the signal response at the output of the 'aggressor' line of the circuit models in Figure 2(A) and 2(B). Ringing is either pronounced or subdued depending on the even or odd mode of current propagation in the aggressor and victim wires. The repeated 'overshoots' and 'undershoots' adversely affect the delay of the line as it increases the **'settling-time'** of the signal response. In addition to the rise time (t_r) of the signal, the settling time (t_s) has to be accounted to obtain the actual wire delay (t_d) [11], [10].

$$t_d = t_r + t_s \tag{1}$$

In our work, we find the best candidate route for each of the nets such that the chosen route has the least 'ringing' and has minimum adverse impact on the neighboring wires.

***Circuit and Central Moment metric*:** The RC Elmore delay model used in previous routing papers is insufficient to account for

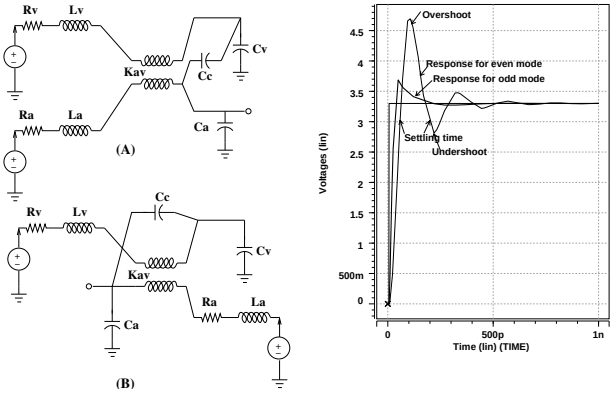

Figure 2: (A) Even-mode (B) odd-mode interaction (C) Ringing phenomenon in output waveform response

the high frequency inductive parasitics of the interconnects and can lead to inaccuracy. In order to account for the self and mutual inductive effects we resort to higher order moments of the impulse response to create an accurate delay approximation. The Laplace transform of the time-domain impulse response *h(t)* is given by [12],

$$H(s) = \int_0^\infty h(t)\, e^{-st}\, dt \tag{2}$$

Using Taylor's series expansion of exponential function e^{-st}, we get,

$$H(s) = \int_0^\infty h(t)\, [1 - st + \frac{1}{2}s^2t^2 - \frac{1}{6}s^3t^3 + ...]\, dt \tag{3}$$

$$H(s) = \sum_{i=0}^{\infty} \frac{(-1)^i}{i!}\, s^i \int_0^\infty t^i h(t)\, dt \tag{4}$$

Expanding a given transfer function (Eqn.5) about $s = 0$ (McLaurin Series) we obtain Eqn.(6).

$$\frac{V_0(s)}{V_i(s)} = H(s) = \frac{b_0 + b_1 s + b_2 s^2 + ... + b_m s^m}{1 + a_1 s + a_2 s^2 + ... + a_n s^n} \tag{5}$$

$$H(s) = m_0 + m_1 s + m_2 s^2 + m_3 s^3 + ... = \sum_{i=0}^{\infty} m_i s^i \tag{6}$$

On comparing Eqn.(4) with Eqn.(6) we find the RLCK circuit moment as the 'q'th coefficient of the impulse response [13],

$$m_q = \frac{(-1)^q}{q!} \int_0^\infty t^q\, h(t)\, dt \tag{7}$$

The concept of ***central moments*** is taken from probability theory and is used in delay characterization [14]. The mean of the impulse response is given by [13]

$$\eta = \frac{\int_0^\infty t h(t)\, dt}{\int_0^\infty h(t)\, dt} = \frac{m_1}{m_0} \tag{8}$$

and the central moments of the impulse response are defined as

$$\mu_k = \int_0^\infty (t - \eta)^k\, h(t)\, dt \tag{9}$$

Using Eqn.(7) and Eqn.(9), the first four central moments are derived as the following [14].

$$\mu_0 = \int_0^\infty (t-\eta)^0 \, h(t)\, dt = m_0 \quad (10)$$

$$\mu_1 = \int_0^\infty (t-\eta)^1 \, h(t)\, dt = \int_0^\infty th(t)\, dt - \eta \int_0^\infty h(t)\, dt = -m_1 - \frac{(-m_1)}{m_0} m_0 = 0 \quad (11)$$

$$Similarly, \mu_2 = 2m_2 - \frac{m_1^2}{m_0} \quad (12)$$

$$and, \mu_3 = -6m_3 + 6\frac{m_1 m_2}{m_0} - 2\frac{m_1^3}{m_0^2} \quad (13)$$

where, μ_2 is a measure of the spread and μ_3 the skewness of the impulse response. Since, the interconnects behave as lossy-transmission lines at high frequencies, there will be an inherent amount of dispersion (μ_2). In contrast, μ_3 can be made to approach the ideal value of zero, which ensures minimum ringing and hence, minimum asymmetry of the waveform response [14]. The ideal condition of $\mu_3 = 0$ with minimum μ_2 gives rise to a "critically-damped" signal response and prevents unnecessary oscillations (overshoots and undershoots). Thus, by making μ_3 as close to zero, we see that the 't_s' term of Eqn.1 reduces to a negligible value and becomes $t_d \rightarrow t_r$. As we also minimize μ_2, we are able to control dispersion of the lossy interconnects. Thus, in addition to the minimum delay we obtain a signal response that is less distorted and preserves signal quality. Hence, in our cost function we resorted to minimization of both μ_2 and μ_3 as the primary objective. The trade-off between ringing and rise-time will be discussed in Section 4.5.

4. PROPOSED METHODOLOGY

We propose a routing methodology that uses the concepts introduced in Section 3 to find the best possible overall routing solution that has the least parasitic interactions and the best ringing and delay trade-off for all the nets. We describe each of the six steps in our approach and their objectives below.

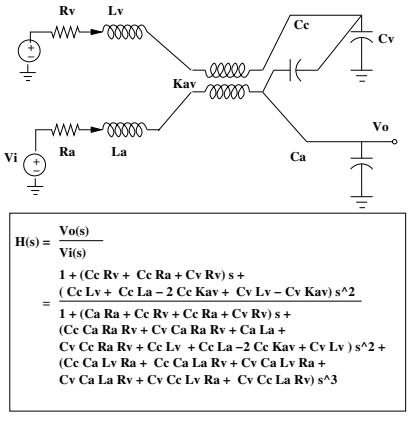

Figure 3: Transfer function of 2 interacting wires in even mode

4.1 Transfer Function Generation

We demonstrate a simple example in Figure 3 to generate the moment-metrics, μ_2 and μ_3 of two interacting wires, where the top wire is the victim and the bottom wire is the aggressor. The transfer function $H(s)$ of this circuit has been generated using SAPWIN v3.0 and is shown in Figure 3. SAPWIN is essentially a symbolic transfer function generator (V_0/V_i) that generates the transfer function after solving the Kirchoff's node voltage and branch current equations using modified-nodal-analysis (MNA) techniques. The important point to note in the expression of $H(s)$ is the introduction of mutual inductance(K) and coupling capacitance terms(Cc) of the neighboring wires.

The **symbolic** representation of the second and third order moments of this circuit are given in Eqn. (14) and Eqn. (15) respectively.

$$\mu_2 = (Ca^2 + 2CaCc)Ra^2 - 2CvCcRaRv - 2CvKav - 2CaLa \quad (14)$$

$$\mu_3 = (2Ca^3 + 6Ca^2Cc + 6CaCc^2)Ra^3 + (-6CvCc^2Rv + 6CaCc^2Rv)Ra^2 + (12CaCcKav - 12CaCcLa - 6CvCc^2Rv^2 - 6Cv^2CcRv^2 - 6CvKavCc + 6CvCcLv - 6Ca^2La)Ra - 6Cv^2KavRv + 6CvCcLaRv - 6CvKavCcRv \quad (15)$$

In order to come to a reasonable conclusion and an intuitive explanation from such a complex value of μ_2 and μ_3 we assume the capacitance and resistance of the aggressor and the victim wires to be equal, i.e, $Ca = Cv$ and $Ra = Rv$. However, we have used the entire expression of μ_2 and μ_3 and have not imposed the limitation of $Ca = Cv$ and $Ra = Rv$ in our methodology. The corresponding reduced equations are given below.

$$\mu_2 = Ra^2Ca^2 + 2Ra^2CaCc - 2Ra^2CaCc - 2CaKav - 2CaLa$$

$$\Rightarrow \mu_2 = Ra^2Ca^2 - 2Ca(La + Ka) \quad (16)$$

$$\mu_3 = 2Ra^3Ca^3 - 6RaCa^2La - 6Ca^2KavRa$$

$$\Rightarrow \mu_3 = 2Ra^3Ca^3 - 6RaCa^2(La + Kav) \quad (17)$$

From the above Eqn. (16) and (17) we can intuitively infer that μ_2 and μ_3 are always positive when $La, Ka = 0$, which represents lossy lines with "overdamped" response [15]. Also, μ_2 and μ_3 decreases monotonically as the self and mutual inductance values increases. We also notice that the effective inductance is the sum of $(La+Kav)$ signifying even mode of current propagation in the aggressor and victim wires. We can conclude that, when interconnect self and mutual inductance is not important (as is the case at sub-GHz frequencies) the analysis corresponds to a simple RC model with "overdamped" waveform response. Similarly, $\mu_2 \leq 0$ and $\mu_3 \leq 0$ implies that the interconnects suffer high inductive effects and results in signal distortion in the form of "ringing" as described earlier in Section 3.

***Objective*:** We pre-generate the symbolic transfer function ($H(s)$) of interconnects using SAPWIN, which also accounts for the nearest neighbor mutual inductance and coupling capacitance terms. From this transfer function we obtain the symbolic expressions of μ_2 and μ_3 as shown in Section 3. The different ways an interconnect can interact with its neighboring wire will be discussed below. The symbolic generation of the expressions of μ_2 and μ_3 are a **one-time** process and occur outside the loop of our routing algorithm.

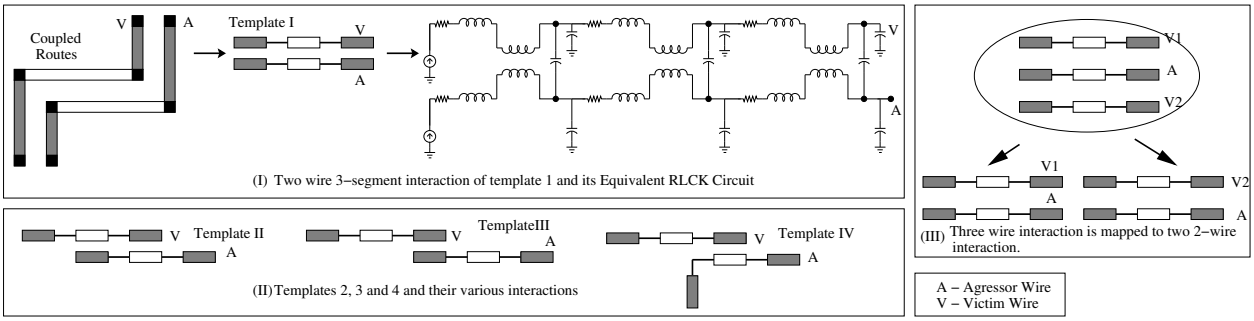

Figure 4: Templates to determine interactions among wires and an example showing the RLCK elements for Template 1

Dynamic evaluation of these symbolic expressions are done within our algorithm as the values of K and Cc changes for different candidate routes of a particular net. This allows us to find the best route with least interaction with nearest neighbors and minimizes μ_2 and μ_3 for that net.

4.2 Templates for Candidate Routes

The above analysis shows that inductive effects play a crucial role in determining the correct delay and output signal response. We have extended the above analysis to generate robust transfer functions for the candidate interconnect structures used in our router. A 1-bend (L-shaped) wire is split into two segments while a 2-bend (Z-shaped) wire is split into three segments to model the nets as a simple distributed RLC network. It is important to note that during the routing process, routing of the current net also affects the waveform response of its neighboring "victim" nets.

In order to capture accurate parasitic interactions between the aggressor and the victim wires we have generated the required templates (Figure 4) that cover the various ways by which the 1-bend and 2-bend interconnects can interact with each other. The L-shaped route is a subset of Z-shaped route, hence we generate the templates with only Z-shaped nets in mind. By reducing R,L and C of any of the end segments to zero of a Z-shaped route we can produce the required template for a L-shaped net. The corresponding transfer functions are pre-generated for these templates and are used on the fly as deemed necessary, based on the way the candidate routes for the current net interacts with its neighboring wires. Figure 4(III) demonstrates how a 3-wire interaction for the aggressor net (A) is broken down into two, 2-wire interaction. The transfer function for each of the corresponding 2-wire interaction is then used to determine the second and third-order central moments and finally combined to generate the cumulative μ_2 and μ_3. For the 3-wire case we have assumed that the victim wires at the top (V1) and the bottom (V2) do not interact with each other.

These four primitive templates or their derived reduced forms are used to capture the various possible interactions of the 1-bend and 2-bend wires with other neighboring wires.

***Objective*:** The templates account for the various ways the L-shaped and the Z-shaped nets can couple with other L-shaped and Z-shaped wires. The templates and their symbolic transfer functions are pre-generated using SAPWIN. Using these transfer functions the central moments (μ_2 and μ_3) for each of the templates are symbolically derived using the symbolic Maple toolbox of Matlab and are stored in a library. During the routing of a net our moment-driven routing algorithm chooses the required template from the library and evaluates its corresponding moments dynamically based on the values of R, L, C, Cc and K.

4.3 Estimation of R,L,C,K

We have estimated the values of resistance, capacitance, inductance, coupling capacitance and mutual inductances of the wire segments based on the wire geometry. The following analytical expressions are used for the estimation of these parasitics for quick and accurate evaluation of these electrical parameters. Resistance (R) is calculated as in Eqn. 18. We did not consider the skin-effect of the wire as the skin-depth of Aluminium between 3-10GHz, ranges between 1.6μ - 0.87μ, which is greater than the wire thickness of 0.4μ considered in this work. The analytic equations used to calculate self and coupling capacitance (C, Cc) of the wire is given in Eqn. 19 and Eqn. 20 respectively. The values of area, perimeter and fringe capacitance are derived from technology parameters. The accuracy of the self and mutual inductance(L, K) formulas with field-solver simulations are documented in [16] and are given by Eqn. 21 and Eqn. 22 respectively.

$$R = \frac{\rho}{t}(\frac{l}{w}) \quad (18)$$

$$C = (area\ cap) \times l \times w + (perim\ cap) \times 2(l + w) \quad (19)$$

$$Cc = (fringe\ cap) \times \frac{overlap\ length}{d} \quad (20)$$

$$L_{self} = \frac{\mu_0}{2\pi}[l \ln(\frac{2l}{w+t}) + \frac{l}{2} + 0.2235(w + t)] \quad (21)$$

$$K = \frac{\mu_0 l}{2\pi}[\ln(\frac{2l}{d}) - 1 + \frac{d}{l}] \quad (22)$$

where, 'l', 'w' and 't' are the length, width and thickness of the conductor and 'd' is the distance of separation of the coupled wires. We did not consider the coupling parasitics between orthogonal wires and have used other expressions given in [16] for calculating mutual inductance of two parallel wires with unequal length.

4.4 Route Cost Function

The costfunction is formulated with the knowledge that routing of a particular net connecting two pins at any instance of the routing process may affect the signal response and delay of its neighboring wires. During the route determination process of a net, we consider several possible candidate solutions for that net.

Let us consider that there are 'n' nets that have to be routed and at a particular instance the 'i'th net needs to be placed. The following steps illustrate the cost function formulation.

1. For each of the 'k' candidate routes of net 'i' symbolic expressions of μ_2 and μ_3 are evaluated using estimated values of R,L,C,Cc and K.

2. The μ_2's and μ_3's of all the affected nets (victims) that have already been routed are re-evaluated.

3. For each candidate of net 'i', we compute the overall standard deviation of the already routed and the current net as given below. This gives the cumulative cost (C_{cost}) for each candidate route and is a measure of the overall dispersion and skewness from the ideal value ($\mu_{2id} = 0$ and $\mu_{3id} = 0$).

$$C_{cost} = \sqrt{\frac{\sum_{n=1}^{i}(\mu_2^n - \mu_{2id})^2}{i}} + \sqrt{\frac{\sum_{n=1}^{i}(\mu_3^n - \mu_{3id})^2}{i}}$$

4. Store the values of the cumulative cost function for each candidate route.

5. Select the candidate route having the least cumulative cost and add to the list of routed nets.

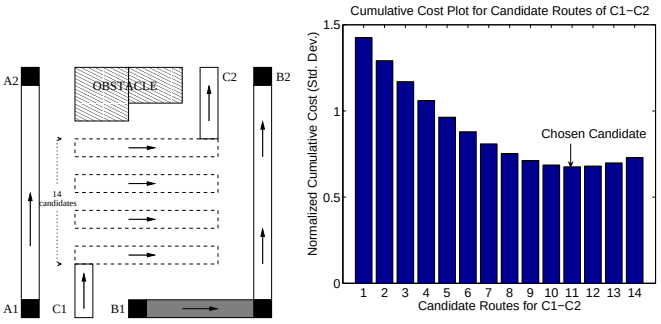

Figure 5: (A) Possible Candidate Routes of C1C2 (B) Normalized Cumulative Cost (Std. Dev) for Candidate Routes (C1C2)

The cost funtion thus gives a snapshot of the cumulative performance in terms of second and third-order central moments of all the nets up to the current net 'i'.

Figure 5(A) and 5(B) illustrates the cost function flow. Out of the 14 candidates, the cost function chooses candidate 11 as the routing solution for net C1C2, which yields the least cumulative cost. This implies that the chosen candidate obtains the best trade-off between ringing and delay among all other candidates and provides the least distortion to its affected neighbors A1A2 and B1B2.

***Objective*:** The objective of developing such a costfunction can be understood from Section 4.5 below.

4.5 Ringing and Delay trade-off

As stated in Section 3, minimizing the second central moment μ_2, results in reduction of the spread (dispersion) of the waveform response thereby obtaining an output response with quicker rise time (t_r). But, the faster transition results in more ringing and the signal suffers from repeated overshoots and undershoots. Though the rise time may prove to be beneficial the increased settling time adversely affects the signal delay (t_d)[10], [11]. In order to minimize ringing and decrease the settling time delay (t_s) we also try to minimize the third central moment (μ_3) sacrificing a bit on the transition rate of the signal. Hence, we formulate our costfunction as given below.

$$S_{mom} = \sqrt{\frac{\sum_{n=1}^{i}(\mu_2^n - \mu_{2id})^2}{i}} \quad (23)$$

$$T_{mom} = \sqrt{\frac{\sum_{n=1}^{i}(\mu_3^n - \mu_{3id})^2}{i}} \quad (24)$$

$$C_{cost} = S_{mom} + \alpha\, T_{mom} \quad (25)$$

S_{mom} and T_{mom} in Eqn. 23 and Eqn. 24 represents the overall standard deviation of all the affected victim nets that have already been routed and the current net 'i'. Note that we have used normalized values of S_{mom} and T_{mom} to get C_{cost}.

***Objective*:** The final C_{cost} is evaluated by taking a weighted sum of S_{mom} and T_{mom}, which ensures a relative trade-off between ringing and transition delay[14]. The C_{cost} of different candidates of net 'i' are evaluated and the one that yields the minimum cost and closest to the ideal value of 0 is chosen as the best route. In our work we have given equal importance to ringing and delay minimization of a net and have chosen $\alpha = 1$ in Eqn. 25.

4.6 Moment-driven Routing Technique

In our routing methodology (Figure 6) the possible candidate routes of a net are generated similar to the level 0 and level 1 lines of the standard Mikami-Tabuchi algorithm [17], which has been tailored to include our 'moment driven' cost function. As the routing of nets will eventually be guided by our cost function, we did not use a maze router because of its expensive memory requirements and which may not be suitable for routing MCM modules over a large chip area.

Figure 6: Moment Driven Routing Methodology

Inputs:
$P[1..2n]$: List of Pins and Pin Types
$N[1..n]$: List of Ordered Nets
$O[1..k]$: Initial Obstacle List
$sym\_\mu_2[1..4]$: Pre-generated symbolic 2nd order moments
$sym\_\mu_3[1..4]$: Pre-generated symbolic 3rd order moments
Output:
$R[1..n]$: Routing Solution
Begin
RoutedNets = ϕ
for $i \in [1..n]$
$C[1..j] \leftarrow Generate\_Candidate(N[i], O[1..k+i-1])$
for $k \in [1..j]$
$T\_id \leftarrow Choose\_Template(C[k], RoutedNets)$
$Parasitics \leftarrow Calc\_Parasitics(C[k], RoutedNets)$
$(\mu2[k], \mu3[k]) \leftarrow Eval\_Moments(Parasitics, sym\_\mu_2[T\_id], sym\_\mu_3[T\_id])$
end for
$Std\_dev[1..j] \leftarrow CostFunction(\mu2[1..j], \mu3[1..j])$
$R[i] \leftarrow$ Select $C[x]$ with least Std_Dev
$RoutedNets \leftarrow RoutedNets \cup R[i]$
Update Obstacle list O with R[i]
end for
End

Any ordering of nets can be handled by the router and should be given as an input to the program. The direction of signal is also

known at this point as we know the terminals to be either an input, output or a bidirectional pin. For an unidirectional current flow between an input-output pin pair of a net, we follow the principle described in Section 4.4 before, while for a pair of bidirectional pins, the candidate route is chosen by modifying the cost function slightly. In that case, the second and third central moments are evaluated considering the current flow in either direction for each of the candidate routes. The route, which yields the minimum cost in both the cases is selected the winner after doing a cumulative measure of the two moments.

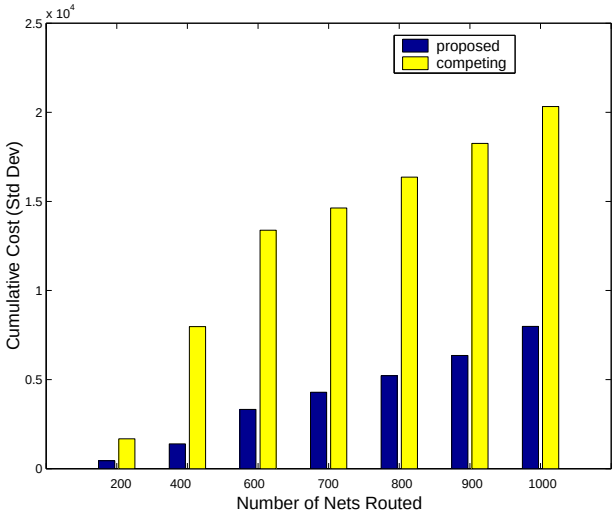

Figure 8: Cumulative cost Comparison of 200, 400, 600, 700, 800, 900 and 1000 nets

We have considered only 2-pin nets that can be connected using either a 1-bend or a 2-bend route. Majority of the nets in a MCM circuit have only two pins. This can be observed from the data given in Table2, of two industrial multi-chip module benchmarks. We see that for mcc1, 75.8% of the total number of nets are 2-pin nets, while for mcc2 it is about 94.11%. We focus on routing these two pin nets using our methodology. Multi-terminal nets can be broken down into a number of two-terminal nets as described by Borah et. al in [18], in their edge-based steiner-tree routing methodology. The resulting two terrminal nets can then be routed using our methodology. The inspiration of using L-shaped and Z-shaped technique find its origin in other related work by Kastner et.al in [1], [3] and by Smey et. al in [2]. A pre-specified step-size is used to generate 'k' possible 2-bend candidate solutions for the current net that needs to be routed. Our implementation is flexible to accommodate other methods to generate candidate solutions as well. For 1-bend candidates, there can be at most two routes (either a upper-L or a Lower-L route) to choose from. As we inspect 'k+2' possible candidates for each of the 'n' nets in our sequential algorithm, the routing complexity is $\Theta(kn)$, in contrast to $\Theta(k^n)$ complexity in the method described in [2]. We would also like to point out that the symbolic transfer function generation using SAPWIN is a 'one-time' process for each of the templates and occurs outside the algorithm loop. As we have considered a few RLC segments to model each net, this one-time transfer function generation takes only a few seconds to get generated.

Design rule violations (DRC errors) are automatically eliminated by following the H-V routing technique. In addition, minimum spacing and width rules are accounted for during candidate route generation.

5. EXPERIMENTAL RESULTS

We have randomly distributed pairs of pins in our experiments and have routed the terminal pairs using our moment-driven line-search algorithm. Figure 7(A) shows the completed route of one such randomly distributed 200 pair of terminals. We have formulated our costfunction based on the second and third order central moments (μ_2 and μ_3). During moment evaluation we have accounted for the nearest neighbor capacitive and inductive coupling parasitics as well as the self resistance, capacitance and inductance of each net.

We compare our routing methodology to a standard line-search algorithm. For the competing approach, we picked the first route found by the router, while in our approach the nets are selected based on our moment-driven costfunction. Figure 7(B) and 7(C) shows the step response of the worst net for the 200 and 600 net routing cases using the two approaches. As the worst net determines the maximum speed of the circuit, we chose to do a comparative analysis on it. We extracted the parasitic elements of the worst net using the quasi-static extractor VPEC [19] and performed Hspice simulation on it. The rise time of the step response is set at 34ps, which means a significant frequency of $0.34/34ps = 10GHz$ [12]. The graphs clearly shows that our method results in better performance for the worst net. While the competing method resulted in either underdamped (more ringing) or overdamped (more delay) waveforms, we were able to obtain a critically-damped response for both the 200 and 600 net routing cases. The proposed method obtains a routing solution based on a costfunction that finds the best trade-off between ringing (μ_3) and delay (μ_2). This ensures a signal response with better signal quality in terms of rise time, settling time, signal overshoots and undershoots. As the competing method is not driven by this costfunction, the routing solution is not guaranteed to be critically-damped and hence can suffer from either a signal underdamp or an overdamp. Similar promising results are obtained also for the 400, 700, 800, 900 and 1000 net cases.

Table 1: Comparison of M(x) = ($\sqrt{\mu_2^2 + \mu_3^2}$) of the worst net and observation between our method and competing approach

No. of Nets	Our Approach	Competing Approach	Improvement in %	Observation from hspice
200	13.31	19.97	33.35	NCD
400	18.26	31.32	41.70	NCD
600	23.05	31.78	27.47	NCD
700	23.91	33.44	28.50	NCD
800	25.69	36.64	29.89	NCD
900	21.83	32.01	31.80	NCD
1000	30.17	42.25	28.59	LOD

NCD : near critically damped, LOD : less overdamp

We measured the cumulative cost (standard deviation) of the routing solution obtained, in separate instances of routing 200, 400, 600, 700, 800, 900 and 1000 nets respectively. We see that the cumulative cost obtained using our method is significantly better than the competing approach as shown in Figure 8. From the fact that the cumulative cost represents the overall signal quality and delay of all the nets and since the proposed technique is driven by a costfunction that finds the best trade-off between ringing and delay we conclude that our approach yields better routes in the presence of

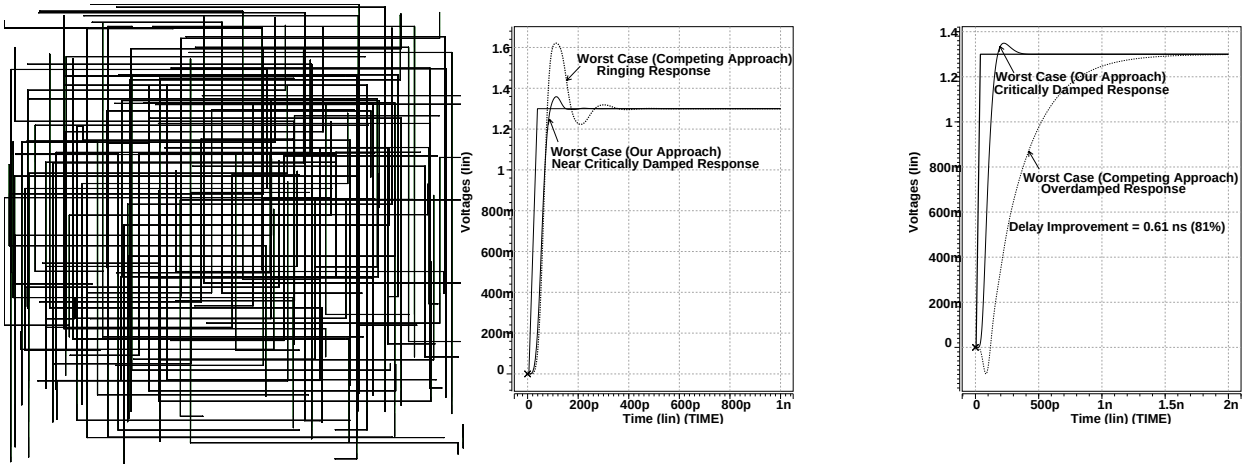

Figure 7: (A) Routed Layout with 200 nets, (B,C) Hspice simulation for the worst net for 200 and 600 net cases

RLCK parasitics compared to traditional approaches.

Figures 9 and 10 shows the plot of the standard deviation of the second and third order central moments of each net for the 400 and the 900 net routing cases. The general trend of the cost of each net is lower in our approach compared to the competing approach. It can also be observed that the cost of the worst net is much higher in the competing approach.

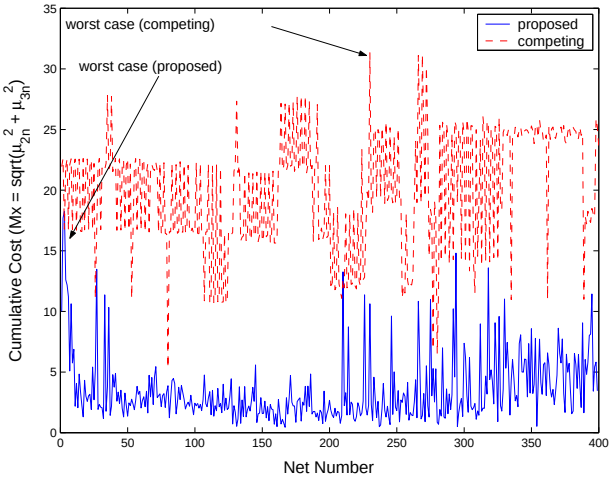

Figure 9: Trend for 400 nets

Table 1 compares standard deviation M(x) = ($\sqrt{\mu_2^2 + \mu_3^2}$) of the worst net between the two approaches for each of the routing cases. The values are normalized for simplicity. We observe that the standard deviation values are much closer to zero in our approach. The relative observation from Hspice simulation shows that the worst net has less overdamp (LOD) or near critically-damped (NCD) response in our method.

The horizontal and vertical segments of the routes are in different metal layers and the rules required to avoid DRC violations are implemented in the routing methodology. The routing algorithm has been developed using C++, and we have used SAPWIN to generate

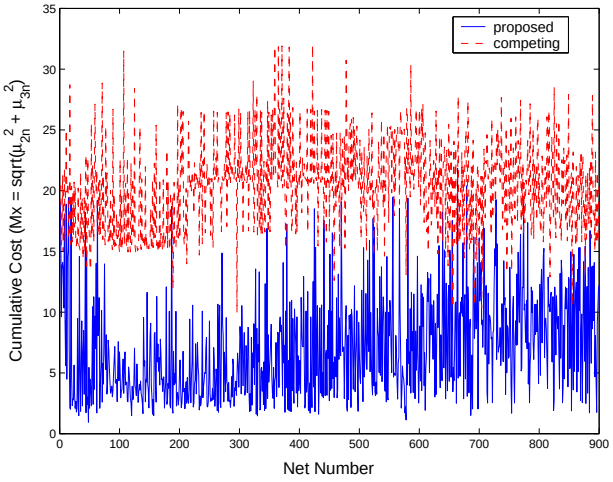

Figure 10: Trend for 900 nets

the one-time symbolic transfer functions for the templates used.

5.1 Scalability of the Results

We notice that the improvement percentage obtained for the various nets in Table 1 does not scale with the increase in the number of nets. To support this counter argument it must be stated that in order to make the benchmarks more stringent, we kept the area of the routing region for all the benchmarks constant. It is obvious that as the wiring density increases in the same routing region, the space available for routing benchmarks with large number of nets effectively decreases. In reality, for MCM circuits as the number of nets increases, the chip area and the area of the routing region increases too (Table 2). Thus, in those cases we can expect proper scalability with the increase in the number of nets. We could have performed our experiments on these industrial MCM benchmark circuits, but we were not able to procure the netlists. Thus, in order to make the routing problem more intensive and stringent, and to circumvent the unavailability of these benchmarks we did not increase the

routing area in our benchmarks, to make the problems more difficult. Table 2, shows the net distribution and the chip area of two industrial MCM modules taken from Microelectronics and Computer Technology Corporation(MCC) and given in [10],[20]. The benchmark mcc2 in particular represents a supercomputer with 37 very high speed integrated circuit gate arrays.

Table 2: Net distribution and substrate area of mcc1 and mcc2

	Total Nets	2-pin Nets	Substrate Size (mm^2)
mcc1	802	608	45 x 45
mcc2	7118	6699	152.4 x 152.4

5.2 Discussion about Worst Case Analysis

In our experiments, we have considered a scenario, which is suitable to represent worst case behavior of the routed nets. In this work, we have assumed the signals in all the wires to switch at the same time. Some recent trends highlight the importance of stochastically modeling the switching of the signal wires, citing that in reality not all wires switch at the same time and considering simultaneous switching might lead to the underestimation of the rise time of the signals. Though much attention is being given to incorporate this stochastic switching distribution, we in this work consider the worst case scenario with a logical reasoning that the routing obtained under this condition will also be effective and will perform better under stochastic switching. We plan to investigate this aspect in the future.

6. CONCLUSION AND FUTURE WORK

Performance-driven routing is increasingly becoming important as circuit and multi-chip-module (MCM) designs progress towards the deep-submicron (DSM) regime. Interconnect parasitic optimization cannot remain restricted to a simple RC or a RLC model. At multi-GHz frequencies the crosstalk among interacting wires become important. In this paper, we have proposed a routing methodology that takes into account the inductive and capacitive coupling parasitics between neighboring wires during the costfunction evaluation of the moment-driven routing process. The proposed approach ensures a routing solution for a number of randomly distributed pin-pairs, which has the least signal distortion and high signal quality. As the waveform response of each of the routed nets is close to the critically-damped condition, the ringing effect and signal delay are also minimized. This minimization is also essential when the inductive effect of long nets produces sharp overshoot in the signal response, which might break the oxide of the gate that it connects to. In contrast a undershoot might cause a logic failure.

In the future, we want to extend this work to guide the routing of multi-bend nets. We would like to implement a robust transfer function generator instead of SAPWIN to create a global template that would be able to capture the different ways two wires can interact and will allow us to do incremental routing with increased number of bends.

7. REFERENCES

[1] R. Kastner, E. Bozorgzadeh and M. Sarrafzadeh. Coupling Aware Routing. In *International ASIC/SOC Conference*, pages 392 – 396, 2000.

[2] R. M. Smey, B. Swartz and P H. Madden. Crosstalk Reduction in Area Routing. In *Design Automation and Test in Europe Conference*, pages 862 – 867, 2003.

[3] R. Kastner, E. Bozorgzadeh and M. Sarrafzadeh. Predictable Routing. In *International Conference on Computer Aided Design*, pages 110 – 113, 2000.

[4] R. T. Hadsell and P. M. Madden. Improved Global Routing through Congestion Estimation. In *Design Automation Conference*, pages 28 – 31, 2003.

[5] J. Cong and P. Madden. Performance Driven Multi-Layer General Area Routing for PCB/MCM Designs. In *Design Automation Conference*, pages 356 – 361, 1998.

[6] T. Ho et. al. A Fast Crosstalk- and Performance-Driven Multilevel Routing System. In *International Conference on Computer Aided Design*, pages 382 – 387, 2003.

[7] J. Lillis et.al. New Performance Driven Routing Techniques With Explicit Area/Delay Tradeoff and Simultaneous Wire Sizing. In *Design Automation Conference*, pages 395 – 400, 1996.

[8] S. Hur, A. Jagannathan and J. Lillis. Timing-Driven Maze Routing. In *Tran. on Computer-Aided Design of Integrated Circuits and Systems*, pages 234 – 241, 2000.

[9] J. Hu and S. Sapatnekar. A Timing-Constrained Simultaneous Global Routing Algorithm. In *Tran. on Computer-Aided Design of Integrated Circuits and Systems*, pages 1025 – 1036, 2002.

[10] J. Cong, C. Koh and P. Maddden. Interconnect Layout Optimization Under Higher Order RLC Model for MCM Designs. In *Tran. on Computer-Aided Design of Integrated Circuits and Systems*, pages 1455 – 1463, 2001.

[11] H. B. Bakoglu. *Circuits, Interconnections, and Packaging for VLSI*. Addison-Wesley, 1990.

[12] C. K. Cheng, J. Lillis, S. Lin and N. Chang. *Interconnect Analysis and Synthesis*. John Wiley & Sons, Inc, 2000.

[13] M. Celik, L. Pileggi and A. Odabasioglu. *IC Interconnect Analysis*. Kluwer Academy Publishers, 2002.

[14] R. Gupta, B. Krauter, L. T. Pileggi. Transmission Line Synthesis via Constrained Multivariable Optimization. In *Tran. on Computer-Aided Design of Integrated Circuits and Systems*, pages 6 – 19, 1997.

[15] Y. Lu et. al. Min/Max On-Chip Inductance Models and Delay Metrics. In *Design Automation Conference*, pages 341–346, 2001.

[16] X. Qi et. al. On-Chip Inductance Modeling and RLC Extraction of VLSI Interconnects for Circuit Simulation. In *Custom Integrated Circuits Conference*, pages 487 – 490, 2000.

[17] K. Mikami and K. Tabuchi. A computer program for optimal routing of printed circuit connectors. In *IFIP*, pages 1475 – 1478, 1968.

[18] M. Borah et. al. An edge-based heuristic for Steiner routing. In *Tran. on Computer-Aided Design of Integrated Circuits and Systems*, pages 1563 – 1568, 1994.

[19] A. Pacelli. A local circuit topology for inductive parasitics. In *International Conference on Computer Aided Design*, pages 208 – 214, 2002.

[20] K. Khoo and J. Cong. An Efficient Multilayer MCM Router Based on Four-Via Routing. In *Tran. on Computer-Aided Design*, pages 1277 – 1290, 1995.